Inorg. Chem. **2005**, *44*, 2766–2773

Transformation of μ_4-Phosphinidenes at an Ru_5 Center: Isolation and Structural Characterization of Hydroxyphosphinidene Cluster Acids, Fluorophosphinidenes, and a Novel μ_5-Phosphide

Ludmila Scoles,[†,‡] Brian T. Sterenberg,[†,§] Konstantin A. Udachin,[†] and Arthur J. Carty*[,†,‡]

Steacie Institute for Molecular Sciences, National Research Council Canada, 100 Sussex Drive, Ottawa, Ontario, Canada K1A 0R6, the Ottawa-Carleton Chemistry Research Institute, Department of Chemistry, University of Ottawa, Ottawa, Ontario, Canada K1N 6N5, and the Department of Chemistry and Biochemistry, University of Regina, Regina, Saskatchewan, Canada S4S 0A2

Received June 9, 2004

Acid hydrolysis of $[Ru_5(CO)_{15}(\mu_4\text{-}PN^iPr_2)]$ (**2**) or protonation of the anionic PO cluster $[Ru_5(CO)_{15}(\mu_4\text{-}PO)]^-$ (**3**) affords the hydroxyphosphinidene complex $[Ru_5(CO)_{15}(\mu_4\text{-}POH)]\cdot\mathbf{1}\cdot[H_2N^iPr_2][CF_3SO_3]$, which cocrystallizes with a hydrogen-bonded ammonium triflate salt. Reaction of $[Ru_5(CO)_{15}(\mu_4\text{-}PN^iPr_2)]$ (**2**) with bis(diphenylphosphino)methane (dppm) leads to $[Ru_5(CO)_{13}(\mu\text{-dppm})(\mu_4\text{-}PN^iPr_2)]$ (**4**). Acid hydrolysis of **4** leads to the dppm-substituted hydroxyphosphinidene $[Ru_5(CO)_{13}(\mu\text{-dppm})(\mu_4\text{-POH})]$ (**5**), which is analogous to **1**, but unlike **1**, can be readily isolated as the free hydroxyphosphinidene acid. Compound **5** can also be formed by reaction of **3** with dppm and acid. The cationic hydride cluster $[Ru_5(CO)_{13}(\mu\text{-dppm})(\mu_3\text{-H})(\mu_4\text{-POH})][CF_3SO_3]$ (**6**) can be isolated from the same reaction if chromatography is not used. Compound **4** also reacts with HBF_4 to form the fluorophosphinidene cluster $[Ru_5(CO)_{13}(\mu\text{-dppm})(\mu_4\text{-PF})]$ (**7**), while reaction with HCl leads to the μ-chloro, μ_5-phosphide cluster $[Ru_5(CO)_{13}(\mu\text{-dppm})(\mu\text{-Cl})(\mu_5\text{-P})]$ (**8**).

Introduction

Phosphinidenes (PR) are important and versatile ligands in organometallic chemistry.[1] The PR group is a powerful polynucleating ligand in metal cluster chemistry that enhances structural integrity and stability through μ_3- and μ_4-face capping coordination.[2] Although cluster-bound phosphinidenes are often inert and used as structural elements, heteroatom-substituted phosphinidenes in clusters can show reactivity at phosphorus.[3−9]

Over the past several years, we have developed an extensive chemistry based on the transformation of functionalized phosphinidenes on metal clusters,[4,5] including the design of a versatile route to phosphorus monoxide (PO) complexes via the acid-catalyzed hydrolysis of P−N bonds in coordinated aminophosphinidenes.[6−9] The $Ru_5(\mu_4\text{-PR})$ clusters have provided a particularly versatile platform for studying the transformations of these ligands, and examples of Ru_5 aminophosphinidenes, fluorophosphinidenes, and phosphorus monoxide clusters have been described.[8,10] The Ru_5 clusters have also been used to form mixed nitrosyl/phosphinidene complexes, allowing us to compare the transformations of phosphorus and nitrogen ligands in the same cluster.[11]

* Author to whom correspondence should be addressed. E-mail: acarty@pco-bcp.gc.ca.
† National Research Council Canada.
‡ University of Ottawa.
§ University of Regina.

(1) Fehlner, T. P. *Inorganometallic Chemistry*; Plenum Press: New York, 1992. Dillon, K. B.; Mathey, F.; Nixon, J. F. *Phosphorus: The Carbon Copy*; John Wiley & Sons, Ltd.: Chichester, U.K., 1998.
(2) Huttner, G.; Knoll, K. *Angew. Chem., Int. Ed. Engl.* **1987**, *26*, 743.
(3) Jordan, M. R.; White, P. S.; Schauer, C. K.; Mosley, M. A., III. *J. Am. Chem. Soc.* **1995**, *117*, 5403. Borg-Breen, C. C.; Bautista, M. T.; Schauer, C. K.; White, P. S. *J. Am. Chem. Soc.* **2000**, *122*, 3952. Wang, W.; Enright, G. D.; Carty, A. J. *J. Am. Chem. Soc.* **1997**, *119*, 12370.
(4) Wang, W.; Corrigan, J. F.; Enright, G. D.; Taylor, N. J.; Carty, A. J. *Organometallics* **1998**, *17*, 427.
(5) Wang, W.; Enright, G. D.; Driediger, J.; Carty, A. J. *J. Organomet. Chem.* **1997**, *541*, 461.
(6) Corrigan, J. F.; Doherty, S.; Taylor, N. J.; Carty, A. J. *J. Am. Chem. Soc.* **1994**, *116*, 9799. Wang, W.; Corrigan, J. F.; Doherty, S.; Enright, G. D.; Taylor, N. J.; Carty, A. J. *Organometallics* **1996**, *15*, 2770. Sterenberg, B. T.; Scoles, L.; Carty, A. J. *Coord. Chem. Rev.* **2002**, *231*, 183−197.
(7) Wang, W.; Carty, A. J. *New J. Chem.* **1997**, *21*, 773.
(8) Yamamoto, J. H.; Udachin, K. A.; Enright, G. D.; Carty, A. J. *Chem. Commun.* **1998**, 2259.
(9) Scoles, L.; Yamamoto, J. H.; Brissieux, L.; Sterenberg, B. T.; Udachin, K. A.; Carty, A. J. *Inorg. Chem.* **2001**, *40*, 6731−6736.
(10) Yamamoto, J. H.; Scoles, L.; Udachin, K. A.; Enright, G. D.; Carty, A. J. *J. Organomet. Chem.* **2000**, *600*, 84.

10.1021/ic040077e CCC: $30.25
Published on Web 03/12/2005

Scheme 1

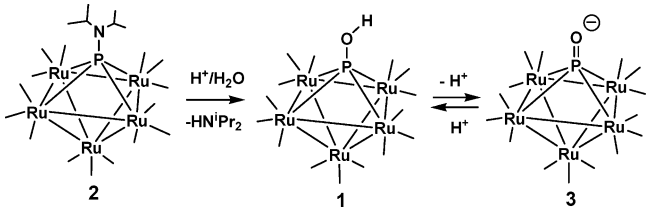

One particularly interesting but poorly documented class of face capping μ-PR ligands is that where the functional group R is OH, namely the hydroxyphosphinidenes. With a single μ_3- or μ_4-POH group bound to a π-acidic $M_n(CO)_m$ cluster core and by analogy to inorganic hydroxyphosphorus compounds, such molecules might be expected to exhibit strongly acidic properties. To date, few such organometallic cluster acids have been characterized, examples being limited to the tetranuclear cluster $Ru_4(CO)_{13}(\mu_3\text{-POH})$[5] and a binuclear rhenium complex bearing a μ_2-POH group.[12]

In this paper, we describe the synthesis of the μ_4-hydroxyphosphinidene cluster $[Ru_5(CO)_{15}(\mu_4\text{-POH})]$ **1** via the acid catalyzed hydrolysis of $[Ru_5(CO)_{15}(\mu_4\text{-PN}^i\text{Pr}_2)]$ **2** and the structure of the strongly hydrogen-bonded association product **1**$[H_2N^i\text{Pr}_2][CF_3SO_3]$. In an effort to modify the reactivity of **2**, we have explored the effect of phosphine substitution at the Ru_5 core to increase the overall cluster electron density and, hence, reduce the acidity of the μ_4-POH group. The success of this strategy is shown by the isolation and structural characterization of $[Ru_5(CO)_{13}(\mu\text{-dppm})(\mu_4\text{-POH})]$, a molecule that contains a non-hydrogen-bonded μ-POH group [dppm = bis(diphenylphosphino)-methane].

Results and Discussion

In our studies on the transformations of substituted PR ligands on Ru_5 clusters, one species that has thus far eluded isolation is the hydroxyphosphinidene $[Ru_5(CO)_{15}(\mu_4\text{-POH})]$ (**1**), which is a plausible intermediate in the transformation of $[Ru_5(CO)_{15}(\mu_4\text{-PN}^i\text{Pr}_2)]$ (**2**) into the anionic PO complex $[H_2N^i\text{Pr}_2][Ru_5(CO)_{15}(\mu_4\text{-PO})]$ (**3**) (Scheme 1). The compound $[Ru_5(CO)_{15}(\mu_4\text{-POH})]$ (**1**) can be readily prepared in solution, either by protonation of $[M][Ru_5(CO)_{15}(\mu_4\text{-PO})]$ (**3**; M = $H_2N^i\text{Pr}_2$ or K) or by hydrolysis of $[Ru_5(CO)_{15}(\mu_4\text{-PN}^i\text{Pr}_2)]$ in the presence of excess acid. However, attempts to crystallize free **1** failed, always resulting in either deprotonation to form **3** or cocrystallization with and hydrogen bonding to a salt. The structure of **1** cocrystallized with the diisopropylammonium triflate salt $[H_2N^i\text{Pr}_2][CF_3SO_3]$ is shown in Figure 1. Selected distances and angles are given in Table 1. The structure reveals hydrogen bonding between the POH ligand and the oxygen of the triflate anion. A peak for the hydrogen atom was located in a difference Fourier map. The O(16)···O(97) distance of 2.639(3) Å, along with a nearly linear O−H···O angle [177(5)°], indicates substantial hydrogen bonding.[13] In the related POH cluster $[Ru_4(CO)_{13}(\mu_3\text{-POH})]$,[5] the solid state structure shows hydrogen bonding to a second molecule of the cluster. This type of interaction is probably less favorable in **1** because of steric interactions between the cluster carbonyl ligands. The P−O distance of 1.590(2) Å is longer than the P−O distance in the related phosphorus monoxide cluster $[H_2NCy_2][Ru_5(CO)_{15}(\mu_4\text{-PO})]$[8] of 1.516(4) Å, which is expected upon protonation of the PO ligand. The core cluster is analogous to several other Ru_5 PR structures previously described[8,10] and consists of five ruthenium atoms arranged in a square-based pyramid. The square base is capped by the phosphorus atom of the POH ligand, resulting in an octahedral arrangement of the core cluster atoms. Each ruthenium atom is bound to three carbonyl ligands. The resulting cluster valence electron count is 74, and with eight metal−metal bonds, the cluster is electron precise. The entire Ru_5P framework contains seven skeletal electron pairs, consistent with a closo M_5E structure.

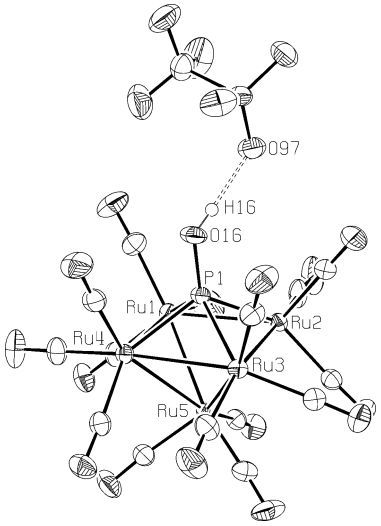

Figure 1. ORTEP diagram of $[Ru_5(CO)_{15}(\mu_4\text{-POH})]$·**1**·$[H_2N^i\text{Pr}_2][CF_3SO_3]$, showing the hydrogen bonding between the POH ligand and the cocrystallized triflate anions. Thermal ellipsoids are shown at the 50% level. The $[H_2N^i\text{Pr}_2]^+$ counterion has been omitted for clarity.

Table 1. Selected Distances and Angles in $[Ru_5(CO)_{15}(\mu_4\text{-POH})]$ **1**·$[H_2N^i\text{Pr}_2][CF_3SO_3]$

P(1)−O(16)	1.590(2)	Ru(1)−Ru(5)	2.7769(3)
Ru(1)−P(1)	2.3657(7)	Ru(2)−Ru(3)	2.8813(3)
Ru(2)−P(1)	2.3247(7)	Ru(2)−Ru(5)	2.8334(3)
Ru(3)−P(1)	2.3462(7)	Ru(3)−Ru(4)	2.8727(3)
Ru(4)−P(1)	2.3160(7)	Ru(3)−Ru(5)	2.8386(3)
Ru(1)−Ru(2)	2.9356(3)	Ru(4)−Ru(5)	2.8502(3)
Ru(1)−Ru(4)	2.8836(3)	O(16)−O(97)	2.639(3)
O(16)−H(1)−O(97)	177(5)		

The difficulty in isolating the "free", non-hydrogen-bonded hydroxyphosphinidene cluster in the solid state and the failure to observe an ^{1}H NMR resonance for the POH ligand in solution even at low temperatures, which is probably due to rapid proton exchange, suggests that the unassociated cluster $[Ru_5(CO)_{15}(\mu_4\text{-POH})]$ is acidic and that hydrogen bonding to the ammonium salt persists in solution. Ready deprotonation of **1** in solution by weak bases such as $HN^i\text{Pr}_2$ to afford **3** confirms this acidity. The structure of

(11) Scoles, L.; Sterenberg, B. T.; Udachin, K. A.; Carty, A. J. *Chem. Commun.* **2002**, 320−321. Scoles, L.; Sterenberg, B. T.; Udachin, K. A.; Carty, A. J. *Can. J. Chem.* **2002**, *80*, 1538−1545.

(12) Ehses, M.; Schmitt, G.; Wolmershäuser, G.; Scherer, O. J. *Z. Anorg. Allg. Chem.* **1999**, *625*, 382.

(13) Taylor, R.; Kennard, O. *Acc. Chem. Res.* **1984**, *17*, 320−326.

Scheme 2

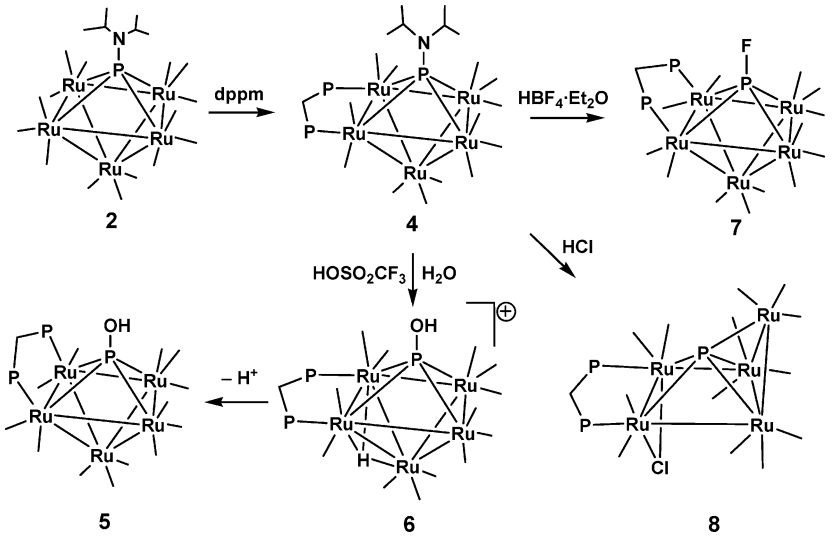

1·$[H_2N^iPr_2][CF_3SO_3]$ (Figure 1) provides a ready explanation for the acid character. The μ_4-POH group is coordinated to four of the five ruthenium fragments in the cluster core, each of which possesses three strong π-acidic CO ligands, which serve to reduce the electron density at the ruthenium centers. The $Ru_5(CO)_{15}$ core is, thus, strongly electron withdrawing toward the POH ligand, rendering the O−H group more acidic. One strategy to reduce this acidity would be to substitute π-acid CO groups on the $Ru_5(CO)_{15}$ cluster core with electron donating phosphine ligands. However, to access phosphine substitution products of **1**, without deprotonating the POH group by the phosphines, it was necessary to approach the problem indirectly, using the aminophosphinidene complex **2** as a precursor.

The complex $[Ru_5(CO)_{15}(\mu_4\text{-}PN^iPr_2)]$ (**2**) reacts with bis(diphenylphosphino)methane ($Ph_2PCH_2PPh_2$, dppm), to form $[Ru_5(CO)_{13}(\mu\text{-dppm})(\mu_4\text{-}PN^iPr_2)]$ (**4**) (Scheme 2). Compound **4** has been structurally characterized. An ORTEP diagram is shown in Figure 2, and selected distances and angles are given in Table 1. The core of the structure consists of five ruthenium atoms arranged in a square-based pyramid with the square face capped by the μ_4-PN^iPr_2 ligand. The structure of **4** is similar to that of **2** and has the same electron count. The diphosphine ligand bridges one edge of the square base, replacing two carbonyl ligands, and is directed away from the aminophosphinidene ligand toward the apical $Ru(CO)_3$ group. Each of the phosphine-bound ruthenium atoms has two additional carbonyl ligands, whereas the other three ruthenium centers have three each. The aminophosphinidene ligand is arranged such that the PNC_2 plane bisects the Ru_4 square approximately parallel to the Ru(1)−Ru(4) and Ru(2)−Ru(3) metal−metal bonds, rather than bisecting the square diagonally, which is more typical of μ_4-aminophosphinidenes.[14] This difference is likely due to the need to avoid steric interactions with the apical CO groups of Ru(1) and Ru(2) as well as with the phenyl substituents of the diphosphine. The P(1)−N(1) distance of 1.688(4) Å is similar to those observed in related μ_4-aminophosphinidenes[9−11,14] and is somewhat shorter than a typical P−N single bond,[15] indicating partial multiple P−N bonding.

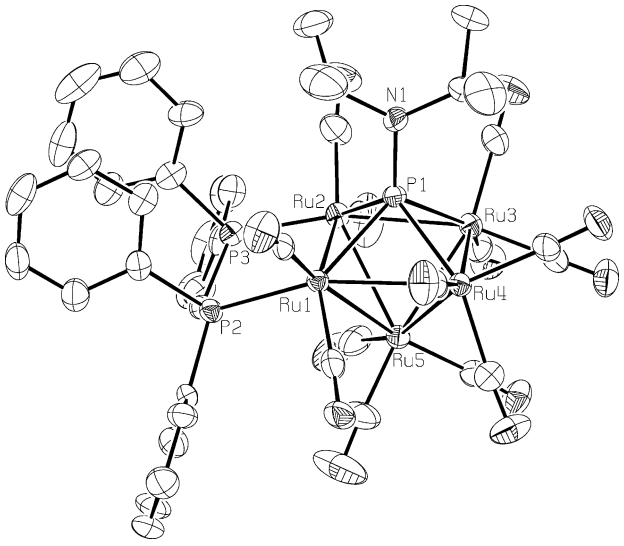

Figure 2. ORTEP diagram of $[Ru_5(CO)_{13}(\mu\text{-dppm})(\mu_4\text{-}PN^iPr_2)]$ (**4**). Thermal ellipsoids are shown at the 50% level, and the hydrogen atoms have been omitted.

The ^{31}P NMR spectrum of **4** consists of a triplet at δ 500 that corresponds to the aminophosphinidene ligand and a doublet at δ 32 corresponding to the dppm ligand. The P−P coupling constant is 38 Hz. The ^1H NMR spectrum shows the expected peaks for dppm phenyl groups and two inequivalent methylene hydrogen atoms, as expected based upon the symmetry of the complex. The two isopropyl groups of the PN^iPr_2 ligand are equivalent in the ^1H NMR spectrum and appear as a septet at δ 4.3 and a doublet at δ 1.4. The IR spectrum shows bands for terminal carbonyl ligands at 2064, 2029, and 2011 cm^{-1}.

Acid hydrolysis of $[Ru_5(CO)_{13}(\mu\text{-dppm})(\mu_4\text{-}PN^iPr_2)]$ (**4**) with triflic acid, followed by thin-layer chromatography, leads to $[Ru_5(CO)_{13}(\mu\text{-dppm})(\mu_4\text{-POH})]$ (**5**). In contrast to

(14) Kahlal, S.; Udachin, K. A.; Scoles, L.; Carty, A. J.; Saillard, J.-Y. *Organometallics* **2000**, *19*, 2251.
(15) Orpen, A. G.; Brammer, L.; Allen, F. H.; Kennard, O.; Watson, D. G.; Taylor, R. *J. Chem. Soc., Dalton Trans.* **1989**, S1.

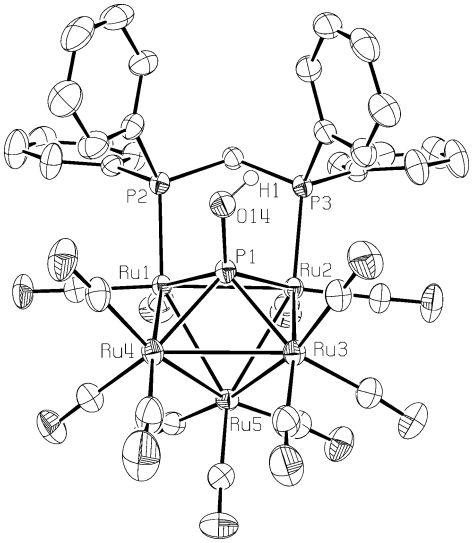

Figure 3. ORTEP diagram of $[Ru_5(CO)_{13}(\mu\text{-dppm})(\mu_4\text{-POH})]$ (**5**). Thermal ellipsoids are shown at the 50% level, and the hydrogen atoms on the dppm ligand have been omitted.

$[Ru_5(CO)_{15}(\mu_4\text{-POH})]$ (**1**), the cluster **5** can readily be isolated free of diisopropylammonium triflate. The ORTEP diagram of the crystal structure is shown in Figure 3. The core structure is the same as that of **1**·$[H_2N^iPr_2][CF_3SO_3]$ with the POH ligand capping the square face of a square-based pyramid of ruthenium atoms. The P−O distance of 1.632(2) Å in **4** is slightly longer than that in **1**·$[H_2N^iPr_2][CF_3SO_3]$ [1.590(2) Å], in which the POH group is hydrogen bonded. This bond-length difference can be attributed to the absence of hydrogen bonding in **5**, but it might also be influenced by the change in cluster electron density that results from replacing two carbonyl groups with dppm. The POH hydrogen atom was located in the Fourier map. In contrast to **4**, the dppm ligand in **5** is positioned well out of the equatorial plane on the same side of the Ru_4 unit as the hydroxyphosphinidene unit, while carbonyl ligands occupy the equatorial positions. This arrangement reflects the much smaller steric size of POH compared to that of the $Ru(CO)_3$ unit on the opposite face and minimizes steric interaction between the dppm and the carbonyl ligands. In contrast, the larger aminophosphinidene ligand in **4** forces the dppm ligand to adopt a more equatorial position. Compound **5** can also be formed by direct reaction of $[K][Ru_5(CO)_{15}(\mu_4\text{-PO})]$ (**3**) with dppm and triflic acid.

The ^{31}P NMR spectrum of the POH cluster **5** shows a triplet at δ 503 for the hydroxyphosphinidene ligand and a doublet δ 25.1 for the dppm ligand. The P−P coupling constant of 11 Hz is smaller than that in **4**, reflecting the relative cis arrangement of the phosphorus ligands in **5**.[16] The P−Ru−P angles in **5** are 92.60(3)° and 93.10(3)°. In **4**, the relationship between the two types of phosphorus ligands is closer to trans with P−Ru−P angles of 138.05(5)°and 131.92(5)°, and the P−P coupling constant is correspondingly larger. No peak for the POH hydrogen in **5** could be located in the ^1H NMR spectrum, which shows only the expected peaks for the dppm phenyl and methylene groups.

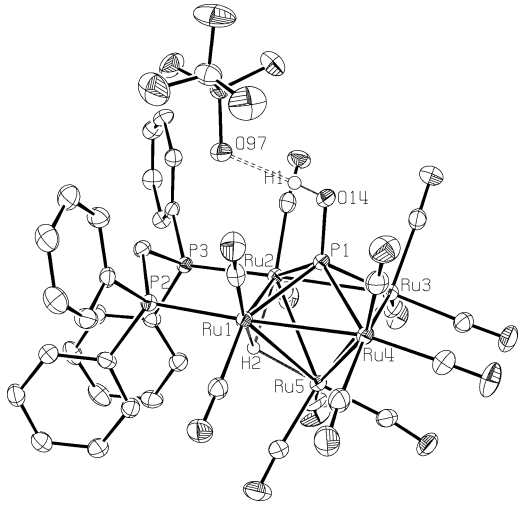

Figure 4. ORTEP diagram of $[Ru_5(CO)_{13}(\mu\text{-dppm})(\mu_3\text{-H})(\mu_4\text{-POH})]$-$[CF_3SO_3]$ (**6**), showing the hydrogen bonding between the POH ligand and the triflate counterion. Thermal ellipsoids are shown at the 50% level, and the hydrogen atoms of the dppm ligand have been omitted.

The acidity of $[Ru_5(CO)_{13}(\mu\text{-dppm})(\mu_4\text{-POH})]$ (**5**) was measured using an acid−base equilibrium with PCy_3 as the base. Equilibrium concentrations were measured using ^{31}P NMR.[17] The pK_a value for **5** is 9.5 ± 0.5 (aqueous scale), similar to that of phenol (pK_a = 10.0). A comparable organometallic acid is the hydride complex $[Ru(H)_2Cp(dmpe)]$ (pK_a = 9.3).[18] These results confirm that the hydroxyphosphinidene cluster **5** is a moderately strong acid, although it is weaker than inorganic phosphorus acids such as H_3PO_4.

In the absence of a chromatographic workup, a different cluster $[Ru_5(CO)_{13}(\mu\text{-dppm})(\mu_3\text{-H})(\mu_4\text{-POH})][OSO_2CF_3]$ (**6**) can be isolated from the above reactions. The ^{31}P NMR spectrum showed a peak at δ 497, in the expected region for a POH ligand. The ^1H NMR showed peaks attributable to the dppm ligand and a metal hydride that appears at δ −18 as a broad singlet. At −80 °C, an additional peak also appears at δ 10.4 that can be assigned to the POH ligand. An ORTEP diagram of the cation is shown in Figure 4. The core of the cluster is the same as that of **5**, with a square-based pyramid of ruthenium atoms capped on the square face with a POH ligand. The POH hydrogen was located in the Fourier map and then placed in an idealized position but allowed to rotate freely about the PO bond. Its final position, and the position of the triflate counterion, clearly indicates the presence of hydrogen bonding between it and the triflate anion. In contrast to that in **5**, the dppm ligand in **6** occupies the equatorial position. This arrangement is necessary to accommodate the hydrogen bonding to the counterion. The hydride ligand was readily located in the Fourier map and bridges the triangular face of the square-based pyramid immediately adjacent to the bridging dppm ligand. The PO distance of 1.606(3) Å is, as expected, shorter than that in **5** and similar to that in **1**·$[H_2N^iPr_2][CF_3SO_3]$.

(16) Jameson, C. J. In *Phosphorus-31 NMR Spectroscopy in Stereochemical Analysis*; Verkade, J. G., Quin, L. D., Eds.; VCH: Deerfield Beach, FL, 1987.

(17) Jessop, P. J.; Morris, R. H. *Coord. Chem. Rev.* **1992**, *121*, 155−284.

(18) Chinn, M. S.; Heinekey, D. M. *J. Am. Chem. Soc.* **1987**, *109*, 5865−5867.

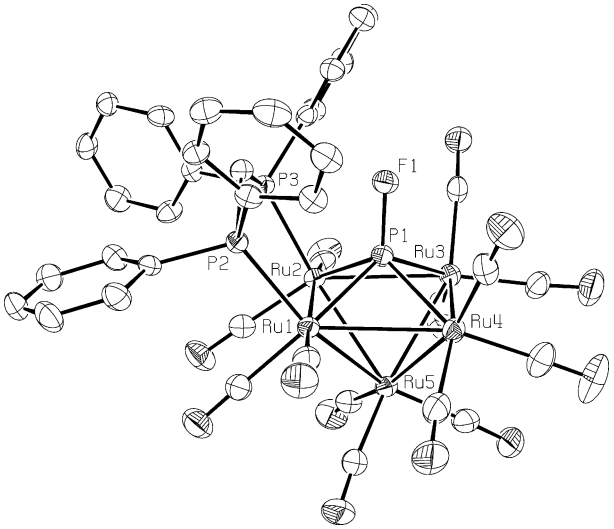

Figure 5. ORTEP diagram of $[Ru_5(CO)_{13}(\mu\text{-dppm})(\mu_4\text{-PF})]$ (**7**). Thermal ellipsoids are shown at the 50% level, and the hydrogen atoms have been omitted.

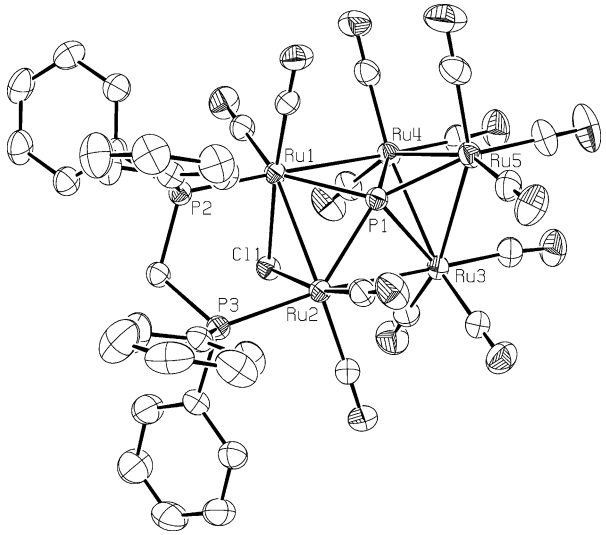

Figure 6. ORTEP diagram of $[Ru_5(CO)_{13}(\mu\text{-dppm})(\mu\text{-Cl})(\mu_5\text{-P})]$ (**8**). Thermal ellipsoids are shown at the 50% level, and the hydrogen atoms have been omitted.

Table 2. Selected Distances in $[Ru_5(CO)_{13}(\mu\text{-dppm})(\mu_4\text{-PN}^i\text{Pr}_2)]$ (**4**), $[Ru_5(CO)_{13}(\mu\text{-dppm})(\mu_4\text{-POH})]$ (**5**), $[Ru_5(CO)_{13}(\mu\text{-dppm})(\mu_3\text{-H})(\mu_4\text{-POH})][OSO_2CF_3]$ (**6**), and $[Ru_5(CO)_{13}(\mu\text{-dppm})(\mu_4\text{-PF})]$ (**7**)

	4	**5**	**6**	**7**
P(1)−N(1)	1.688(4)			
P(1)−O(14)		1.632(2)	1.606(3)	
P(1)−F(1)				1.621(2)
Ru(1)−P(1)	2.384(1)	2.3417(7)	2.3614(11)	2.303(1)
Ru(2)−P(1)	2.356(1)	2.3346(7)	2.3524(11)	2.322(1)
Ru(3)−P(1)	2.424(1)	2.3523(8)	2.3297(11)	2.306(1)
Ru(4)−P(1)	2.381(1)	2.3583(8)	2.3433(11)	2.329(1)
Ru(1)−P(2	2.332(1)	2.3088(8)	2.3356(11)	2.307(1)
Ru(2)−P(3)	2.355(1)	2.2970(8)	2.3433(11)	2.2934(9)
Ru(1)−Ru(2)	2.9428(6)	2.8784(3)	2.9457(5)	2.8796(4)
Ru(1)−Ru(4)	2.8578(6)	2.8965(3)	2.9057(5)	2.9435(4)
Ru(2)−Ru(3)	2.8389(6)	2.9221(3)	2.9201(5)	2.9138(4)
Ru(3)−Ru(4	2.8876(6)	2.9218(3)	2.9080(5)	2.9648(5)
Ru(1)−Ru(5)	2.8656(6)	2.8926(3)	2.9281(5)	2.8538(4)
Ru(2)−Ru(5)	2.9185(6)	2.8462(3)	2.9631(5)	2.8538(4)
Ru(3)−Ru(5)	2.8112(6)	2.8092(3)	2.8353(5)	2.8143(4)
Ru(4)−Ru(5)	2.8742(6)	2.7879(3)	2.8625(5)	2.7875(5)
P(1)−Ru(1)−P(2)	138.05(5)	92.60(3)	127.25(4)	91.52(3)
P(1)−Ru(2)−P(3)	131.92(5)	93.10(3)	128.80(4)	89.40(3)

The hydrolysis of $[Ru_5(CO)_{13}(\mu\text{-dppm})(\mu_4\text{-PN}^i\text{Pr}_2)]$ (**4**) has also been investigated with other acids. Reaction with HBF_4 (with or without water present) leads to the fluorophosphinidene cluster $[Ru_5(CO)_{13}(\mu\text{-dppm})(\mu_4\text{-PF})]$ (**7**), effectively cleaving the P−N bond with HF. This reactivity is consistent with that seen in the reactions of $[Ru_4(CO)_{13}(\mu_3\text{-PN}^i\text{Pr}_2)]$ and $[Ru_5(CO)_{15}(\mu_4\text{-PN}^i\text{Pr}_2)]$ (**2**) with $HBF_4\cdot Et_2O$.[7,10] Compound **7** can be readily characterized by IR and NMR. The PF ligand appears in the ^{19}F NMR spectrum as a doublet of triplets at δ 8.7, showing a large one-bond P−F coupling constant of 1076 Hz, as well as a long-range coupling constant of 20 Hz to the dppm phosphorus atoms. In the ^{31}P NMR spectrum, the PF ligand appears as a doublet of triplets at δ 539, showing the large one-bond P−F coupling constant, as well as a long-range P−P coupling constant of 31 Hz. The resonance for the dppm ligand appears at δ 28.5 as a doublet. The long-range P−F coupling expected on the basis of the ^{19}F spectrum is masked by the broadness of the peaks in the ^{31}P spectrum.

The X-ray structure of **7** (Figure 5 and Table 2) reveals that the structure is analogous to those of **4** and **5**. In **7**, the dppm ligand adopts a conformation similar to that observed in **5**, in which the ligand is above the equatorial plane on the same side as the μ_4-PF ligand. This arrangement reflects the similar size of the PF and POH groups. A comparison of the Ru−P distances to those of the μ_4-phosphinidene ligands (Table 2) shows that increasing the electronegativity of the substituent leads to shorter M−P bonds. This change can be attributed to an increase in metal to phosphorus π back bonding as the electronegativity of the phosphorus substituent increases.[9]

In contrast to the reaction with $HBF_4\cdot Et_2O$, HCl addition led to the μ-chloro, μ_5-phosphide cluster $[Ru_5(CO)_{13}(\mu\text{-dppm})(\mu\text{-Cl})(\mu_5\text{-P})]$ (**8**). The ORTEP diagram of **8** is shown in Figure 6. Selected distances and angles are given in Table 3. The structure consists of four ruthenium atoms arranged in a square, with the fifth ruthenium atom bridging one edge of the square. The angle between the square and the triangle thus formed is 84.07(1)°. The phosphide atom bridges all five ruthenium atoms, forming a nearly symmetrical interaction with the four atoms of the square (Ru−P = 2.363, 2.321, 2.313, and 2.345 Å). The distance to the fifth Ru atom is slightly shorter at 2.233 Å. The chloro ligand bridges the opposite edge of the square from the fifth ruthenium atom on the opposite side of the square. The dppm ligand bridges the same edge as the chloride in the equatorial plane of the ruthenium square. In addition to bridging the chloro and dppm groups, these two ruthenium atoms each have two terminal carbonyl ligands, while the other three ruthenium atoms have three terminal carbonyls each. The resulting electron count is 78, with the phosphide contributing all of its five valence electrons and the bridging chloride functioning as a three-electron donor. The higher electron count compared to that of the μ_4-phosphinidene clusters results in

Table 3. Selected Distances and Angles in $[Ru_5(CO)_{13}(\mu\text{-dppm})(\mu\text{-Cl})(\mu_5\text{-P})]$ (**8**)

Ru(1)−P(1)	2.3455(6)	Ru(2)−P(3)	2.4107(7)
Ru(2)−P(1)	2.3634(6)	Ru(1)−Ru(2)	2.8738(3)
Ru(3)−P(1	2.3208(7)	Ru(1)−Ru(4)	3.0019(3)
Ru(4)−P(1)	2.3129(7)	Ru(2)−Ru(3)	3.0147(3)
Ru(5)−P(1)	2.2333(6)	Ru(3)−Ru(4)	2.9230(3)
Ru(1)−Cl(1)	2.4491(6)	Ru(3)−Ru(5)	2.8878(3)
Ru(2)−Cl(1	2.4342(6)	Ru(4)−Ru(5)	2.8767(3)
Ru(1)−P(2)	2.3451(7)		
P(2)−Ru(1)−P(1)	131.25(2)	Ru(4)−P(1)−Ru(2)	125.35(3)
P(1)−Ru(2)−P(3)	140.86(2)	Ru(3)−P(1)−Ru(2)	80.12(2)
P(1)−Ru(1)−Cl(1)	88.41(2)	Ru(1)−P(1)−Ru(2)	75.221(19)
P(1)−Ru(2)−Cl(1)	88.35(2)	Ru(2)−Cl(1)−Ru(1)	72.100(17)
P(2)−Ru(1)−Cl(1)	90.56(2)	Ru(4)−Ru(5)−Ru(3)	60.937(7)
P(3)−Ru(2)−Cl(1)	84.23(2)	Ru(3)−Ru(4)−Ru(1)	90.235(8)
Ru(5)−P(1)−Ru(4)	78.49(2)	Ru(2)−Ru(1)−Ru(4)	89.969(8)
Ru(5)−P(1)−Ru(3)	78.68(2)	Ru(1)−Ru(2)−Ru(3)	90.924(8)
Ru(4)−P(1)−Ru(3)	78.22(2)	Ru(5)−Ru(3)−Ru(4)	59.344(8)
Ru(5)−P(1)−Ru(1)	140.63(3)	Ru(5)−Ru(3)−Ru(2)	95.355(8)
Ru(4)−P(1)−Ru(1)	80.24(2)	Ru(4)−Ru(3)−Ru(2)	88.792(8)
Ru(3)−P(1)−Ru(1)	128.25(3)	Ru(5)−Ru(4)−Ru(3)	59.719(7)
Ru(5)−P(1)−Ru(2)	143.45(3)	Ru(5)−Ru(4)−Ru(1)	94.321(8)

the more open structure observed for **8** and two fewer Ru−Ru bonds.

The ^{31}P NMR spectrum of **8** shows a triplet for the phosphide ligand at δ 803. A doublet at δ 28 corresponds to the dppm ligand. The P−P coupling constant of 52 Hz is substantially higher than in any of the other complexes and reflects the transoid arrangement of the phosphide and phosphine ligands in **8**. The extreme low-field shift of the phosphide resonance is not unusual for semiencapsulated phosphide ligands.[19,20]

The semiencapsulated μ_5 coordination of the phosphide atom in **8** appears to be quite unusual. Only two five-coordinate phosphide clusters of group 8 metals have previously been described, one of ruthenium[21] and another of iron.[22] In addition, a gold cluster,[23] a nickel cluster,[24] and mixed iron−gold clusters[25] with μ_5-P ligands are known. The coordination mode of the phosphorus atom in **8**, which caps a square of ruthenium atoms and forms an additional bond with the fifth, edge-bridging ruthenium atom, appears to be unique. The previous Ru and Fe complexes contain a more open geometry in which the phosphorus atom bridges a triangle of metal atoms and forms additional bonds to two other metal atoms, which are connected in a chain to the triangle by single metal−metal bonds. In both of these cases, the interaction with one of the five metals is substantially weaker. Coordination of a bare phosphorus atom to six transition metals is much more common, and several examples of Ru,[20,26] Os,[27] and Co[19,28] μ_6-phosphide coordination have been described. Triply and quadruply bridging phosphide ligands are also relatively common.[29]

The difference between HCl and HF addition can be attributed to the nature of the base. The softer chloride anion coordinates to the metals, while the harder fluoride binds preferentially to phosphorus. The dppm ligand seems to be important in maintaining cluster integrity in the formation of **8**. Reactions of analogous aminophosphinidene clusters without dppm with HCl led to cluster fragmentation.

Conclusion

Replacement of π-acceptor carbonyl ligands with a donor phosphine ligand results in a reduction of the acidity of the μ_4-POH ligand. The sensitivity of this ligand to the overall cluster density is not surprising given that the phosphorus atom forms an integral part of the cluster core. The alteration of cluster electron density has allowed the isolation of the targeted μ_4-POH cluster $[Ru_5(CO)_{13}(\mu\text{-dppm})(\mu_4\text{-POH})]$. The presence of the chelating diphosphine ligand also enhances cluster integrity. A novel example of a μ-chloro, μ_5-phosphide cluster $Ru_5(CO)_{13}(\mu\text{-dppm})(\mu\text{-Cl})(\mu_5\text{-P})$ has also been characterized.

Experimental Section

General Comments. Reactions were carried out under an atmosphere of dry nitrogen. Dichloromethane and hexane were appropriately dried before use. The reagents bis(diphenylphosphino)methane, triflic acid, tetrafluoroboric acid, and hydrochloric acid were purchased from Strem Chemicals and Aldrich and used without any further purification. The compounds $[Ru_5(CO)_{15}(\mu_4\text{-}PN^iPr_2)]$ and $[K][Ru_5(CO)_{15}(\mu_4\text{-PO})]$ were synthesized by known procedures.[10] Preparative thin-layer chromatography was carried out using silica gel plates (60 A F_{254}) (Merck, 0.25 mm). The ^{1}H and ^{31}P NMR spectra were recorded on a Bruker DRX-400 spectrometer. Elemental analyses were carried out by Guelph Chemical Laboratories, Guelph, Ontario, Canada.

Preparation of Compounds. a. Synthesis of $[Ru_5(CO)_{15}(\mu_4\text{-POH})]\cdot 1\cdot[H_2N^iPr_2][CF_3SO_3]$. To a green solution of $[Ru_5(CO)_{15}(\mu_4\text{-}PN^iPr_2)]$ (**2**; 120 mg, 0.113 mmol) in CH_2Cl_2 (10 mL) was added triflic acid CF_3SO_3H (120 μL) and H_2O (120 μL). The reaction flask was briefly evacuated, refilled with nitrogen, and then heated under reflux for 18 h. The reaction mixture was dried over magnesium sulfate and filtered. The solvent was removed and the residue was redissolved in CH_2Cl_2 (2 mL), layered with hexane (2 mL), and cooled to −30 °C for 2 days, resulting in the formation of crystals of $[Ru_5(CO)_{15}(\mu_4\text{-POH})][H_2N^iPr_2][CF_3SO_3]$. Yield: 90 mg, 70%. IR (CH_2Cl_2, ν CO, cm^{-1}): 2058 s, 2028 m. ^{31}P{^{1}H} NMR ($CDCl_3$): δ 520. ^{1}H NMR ($CDCl_3$): δ 3.4 [sept., ^3J(HH) =

(19) Liu, S.-T.; Hu, X.; Chang, F.; Liu, Y.-C.; Ding, E.-R.; Wu, B.-F.; Zhao, Z.-R. *Polyhedron* **2002**, *21*, 1073−1080.
(20) Van Gastel, F.; Taylor, N. J.; Carty, A. J. *Inorg. Chem.* **1989**, *28*, 384.
(21) MacLaughlin, S. A.; Taylor, N. J.; Carty, A. J. *Inorg. Chem.* **1983**, *22*, 1409.
(22) Lang, H.; Huttner, G.; Zsolnai, L.; Mohr, G.; Sigwarth, B.; Weber, U.; Orama, O.; Jibril, I. *J. Organomet. Chem.* **1986**, *304*, 157−179.
(23) Beruda, H.; Zeller, E.; Schmidbaur, H. *Chem. Ber.* **1993**, *126*, 2037−2040.
(24) Fenske, D.; Persau, C. *Z. Anorg. Allg. Chem.* **1991**, *593*, 61.
(25) Sunick, D. L.; White, P. S.; Schauer, C. K. *Inorg. Chem.* **1993**, *32*, 5665−5675.
(26) Frediani, P.; Bianchi, M.; Salvini, A.; Piacenti, F.; Ianelli, S.; Nardelli, M. *J. Chem. Soc., Dalton Trans.* **1990**, 1705. Frediani, P.; Bianchi, M.; Salvini, A.; Piacenti, F.; Ianelli, S.; Nardelli, M. *J. Chem. Soc., Dalton Trans.* **1990**, 165.
(27) Colbran, S. B.; Housecroft, C. E.; Johnson, B. F. G.; Lewis, J.; Owen, S. M.; Raithby, P. R. *Polyhedron* **1988**, *7*, 1759−1765. Colbran, S. B.; Lahoz, F. J.; Raithby, P. R.; Lewis, J.; Johnson, B. F. G.; Cardin, C. J. *J. Chem. Soc., Dalton Trans.* **1988**, 173. Colbran, S. B.; Hay, C. M.; Johnson, B. F. G.; Lahoz, F. J.; Lewis, J.; Raithby, P. R. *J. Chem. Soc., Chem. Commun.* **1986**, 1766.
(28) Chini, P.; Ciani, G.; Martinengo, S.; Sironi, A. *J. Chem. Soc., Chem. Commun.* **1979**, 188. Hu, X.; Liu, Q.-W.; Liu, S.-T.; Zhang, L.-P.; Wu, B.-S. *J. Chem. Soc., Chem. Commun.* **1994**, 139.
(29) Di Vaira, M.; Stoppioni, P.; Peruzzini, M. *Polyhedron* **1987**, *6*, 351. Scherer, O. J. *Acc. Chem. Res.* **1999**, *32*, 751.

Table 4. X-ray Parameters for Compounds **1**, **4**, **5**, **6**, **7**, and **8**

	1	**4**	**5**
formula	$C_{22}H_{17}N\,O_{19}F_3PSRu_5$	$C_{48.08}H_{45.52}\,NO_{13}P_3Ru_5$	$C_{38}H_{23}O_{14}\,P_3Ru_5$
fw	1224.75	1443.64	1301.82
cryst syst	monoclinic	orthorombic	orthorombic
space group	$P2_1/n$	*P*bcn	$P2_12_12_1$
unit cell			
a (Å)	9.6282(6)	20.126(1)	11.8241(6)
b (Å)	26.152(1)	36.805(3)	17.7276(9)
c (Å)	14.5780(8)	14.237(1)	20.093(1)
β (deg)	94.373(1)	90	90
V (Å^3)	3660.0(4)	10546(1)	4211.7(4)
Z	4	8	4
ρ_{calc} (Mg mm^{-3})	2.223	1.819	2.053
μ (Mo Kα) (mm^{-1})	2.207	1.552	1.931
θ_{max} (deg)	28.73	25.00	28.73
reflns measured	43233	91420	45347
data/restraints/parameters	9452/1/467	9286/27/658	10878/1/634
GOF	1.047	0.985	1.040
R1 and wR2	0.0248	0.0426	0.0209
[$I > 2\sigma(I)$]	0.0529	0.0837	0,0462
R1 and wR2	0.0331	0.0799	0.0240
(all data)	0.0556	0.0983	0.0462
largest peak in final difference map (e Å^{-3})	0.598	0.762	0.668

	6	**7**	**8**
formula	$C_{40}H_{24}\,O_{17}F_3\,P_3SCl_2Ru_5$	$C_{38}H_{22}O_{13}F\,P_3Ru_5$	$C_{39}H_{24}O_{13}P_3\,Cl_3Ru_5$
fw	1534.81	1303.82	1405.19
cryst syst	monoclinic	monoclinic	monoclinic
space group	$P2_1/c$	$P2_1/n$	$P2_1/c$
unit cell			
a (Å)	17.8738(9)	13.9607(9)	17.4150(7)
b (Å)	12.5377(7)	15.263(1)	15.0898(6)
c (Å)	22.309(1)	20.360(1)	17.7268(7)
β (deg)	94.224(1)	108.472(1)	96.954(1)
V (Å^3)	4985.7(5)	4114.8(5)	4624.1(3)
Z	4	4	4
ρ_{calc} (Mg mm^{-3})	2.045	2.105	2.018
μ (Mo Kα) (mm^{-1})	1.805	1.979	1.933
θ_{max} (deg)	29.60	29.61	28.74
reflns measured	61079	51170	54445
data/restraints/parameters	13922/0/645	11565/0/541	11947/0/568
GOF	1.101	0.988	1.029
R1 and wR2	0.0405	0.0370	0.0247
[$I > 2\sigma(I)$]	0.0912	0.0718	0.0618
R1 and wR2	0.0579	0.0663	0.0327
(all data)	0.0962	0.0791	0.0659
largest peak in final difference map (e Å^{-3})	1.869	0.853	0.940

6.4 Hz, C*H*], 1.4 [d, ^3J(HH) = 6.4 Hz, CH_3]. FAB−MS (*m*/*z*): 973.4 [M+], 974−553 [M−*n*CO] (*n* = 1−15). Anal. Calcd for $C_{22}H_{17}NO_{19}\,F_3PSRu_5$: C, 21.58; H, 1.40; N, 1.14. Found: C, 21.79; H, 1.18; N, 1.14.

b. Synthesis of [Ru$_5$(CO)$_{13}$(μ-dppm)(μ-PN^{i}Pr$_2$)] (4). The cluster [Ru$_5$(CO)$_{15}$(μ_4-PN^{i}Pr$_2$)] (90 mg, 0.085 mmol) and dppm (66 mg, 0.170 mmol) were dissolved in CH_2Cl_2 (10 mL). The solution was heated under reflux for 18 h. The solvent was removed in vacuo, and the residue was separated by thin-layer chromatography on silica gel plates using a 50:50 mixture of CH_2Cl_2/hexane as the eluent. [Ru$_5$(CO)$_{13}$(μ-dppm)(μ_4-PN^{i}Pr$_2$)] (**4**) was isolated as a green compound. Crystals were grown from CH_2Cl_2/hexane at −30 °C. Yield: 42 mg, 35%. IR (CH_2Cl_2, ν CO, cm^{-1}): 2064 m, 2029 s, 2011 m. ^{31}P{^{1}H} NMR ($CDCl_3$): δ 500 [t, ^2J(PP) = 38 Hz], 32 [d, ^{2}J(PP) = 37 Hz]. ^{1}H NMR ($CDCl_3$): δ 7.5−7.0 [m, 20H, Ph], 5.14 [dt, 1H, ^2J(HH) = 13 Hz, ^2J(HP) = 12 Hz, PC*H*HP], 4.92 [dt, 1H, ^2J(HH) = 13 Hz, ^2J(HP) = 12 Hz, PCH*H*P], 4.37 [sept., 2H, ^3J(HH) = 7 Hz, C*H*], 1.40 [d, 12H, ^3J(HH) = 7 Hz, CH_3]. Anal. Calcd for $C_{44}H_{36}NO_{13}P_3Ru_5$: C, 38.16; H, 2.62; N, 1.01. Found: C, 38.37; H, 2.14; N, 0. 91.

c. Synthesis of [Ru$_5$(CO)$_{13}$(μ-dppm)(μ_4-POH)] (5). The cluster [K][Ru$_5$(CO)$_{15}$(μ_4-PO)] (100 mg, 0.099 mmol) was dissolved in CH_2Cl_2 (10 mL) and treated with HCl (100 μL, 1 M solution in ether), and then dppm (72 mg, 0.187 mmol) was immediately added. The solvent was removed in vacuo, and the residue was separated using thin-layer chromatography with CH_2Cl_2 as the eluent. A dark green band was isolated, and X-ray quality crystals of [Ru$_5$(CO)$_{13}$-(μ-dppm)(μ_4-POH)] (**5**) were grown from CH_2Cl_2/hexane at −30 °C. Yield: 23 mg, 18%. IR (CH_2Cl_2, ν CO, cm^{-1}): 2098 w, 2069 m, 2036 m, 2020 s, 2001 m. ^{31}P{^{1}H} NMR ($CDCl_3$): δ 503 [t, ^2J(PP) = 11 Hz], 25.1 [d, ^2J(PP) = 11 Hz]. ^{1}H NMR ($CDCl_3$): δ 7.8−7.3 [m, 20H, Ph], 4.68 [dt, 1H, ^2J(HH) = 14 Hz, PC*H*HP, ^2J(HP) = 12 Hz], 4.20 [dt, 1H, ^2J(HH) = 14 Hz, PCH*H*P, ^2J(HP) = 12 Hz]. Anal. Calcd for $C_{38}H_{23}O_{14}P_3Ru_5$: C, 35.06; H, 1.78. Found: C, 35.38; H, 1.80. Acidity measurements on **5** were carried out by dissolving 15 mg of **5** in CD_2Cl_2 with varying amounts of PCy_3 (0.5, 1, or 3 equiv). Because the acid species were in rapid exchange with the conjugate bases, relative concentrations were measured using the averaged ^{31}P chemical shift. The total phosphine-to-cluster ratio was measured using integration. Equilibrium

constants K were calculated using the measured concentrations, and pK_a was then calculated using the relationship $pK_a = pK_{eq} - pK_{BH+}$, using a value of 9.7 for pK_{BH+} ($HPCy_3^+$, aqueous scale).[17] The average pK_a value for four experiments was 9.5 ± 0.5.

d. Synthesis of $[Ru_5(CO)_{13}(\mu\text{-dppm})(\mu_3\text{-H})(\mu_4\text{-POH})][CF_3SO_3]$ (6). To a solution of $[Ru_5(CO)_{13}(\mu\text{-dppm})(\mu_4\text{-PN}^i\text{Pr}_2)]$ (**4**) (130 mg, 0.094 mmol) in CH_2Cl_2 (10 mL) was added water (10 μL, mmol) and triflic acid (10 μL, mmol). The resulting solution was stirred for 10 min and then dried over magnesium sulfate and filtered. The solvent was reduced to 2 mL, and an equal amount of Et_2O was added. The resulting solution was kept at −30 °C for 2 days, resulting in the formation of dark green crystals. Yield: 30 mg, 22%. IR (KBr pellet, ν CO, cm^{-1}): 2090 m, 2049 w, 2031 s, 2010 w. $^{31}P\{^1H\}$ NMR ($CDCl_3$): δ 497 [t, ^2J(PP) = 29 Hz], 31.8 [d, ^2J(PP) = 29 Hz]. ^1H NMR ($CDCl_3$): δ 7.8−7.1 [m, 20H, Ph], 6.57 [dt, 1H, ^2J(HH) = 13 Hz, ^2J(HP) = 13 Hz, PC*H*HP], 5.12 [dt, 1H, ^2J(HH) = 13 Hz, ^2J(HP) = 13 Hz, PCH*H*P], −18.0 [br, 1H, μ_3-H], 10.4 [br, POH, −80 °C, CD_2Cl_2]. Anal. Calcd for $C_{39}H_{24}O_{17}F_3SP_3Ru_5$: C, 32.26; H, 1.67. Found: C, 31.98; H, 1.41.

e. Synthesis of $[Ru_5(CO)_{13}(\mu\text{-dppm})(\mu_4\text{-PF})]$ (7). To a green solution of $[Ru_5(CO)_{13}(\mu\text{-dppm})(\mu_4\text{-PN}^i\text{Pr}_2)]$ (**4**; 119 mg, 0.086 mmol) in CH_2Cl_2 (10 mL) was added an excess of HBF_4 (54% in Et_2O, 20 μL, 24 mg, 0.15 mmol). The resulting green solution was stirred at room temperature for a half hour. The solvent was removed in vacuo, and the residue was separated using thin-layer chromatography with 50:50 CH_2Cl_2/hexane as the eluent. Crystals of **7** were grown from 50:50 CH_2Cl_2/hexane at −30 °C. Yield: 30 mg, 27%. IR (CH_2Cl_2, ν CO, cm^{-1}): 2074 m, 2042 m, 2025 s, 2008 m.$^{31}P\{^1H\}$ NMR ($CDCl_3$): δ 539 [dt, ^1J(PF) = 1076 Hz, ^2J(PP) = 31 Hz], 28.5 [d, ^2J(PP) = 31 Hz]. $^{19}F\{^1H\}$ NMR ($CDCl_3$ vs CF_3COOH): δ 8.72 [dt, ^1J(PF) = 1076 Hz, ^3J(PF) = 20 Hz]. ^1H NMR ($CDCl_3$): δ 7.5−7.3 [m, 20H, Ph], 4.46 [dt, 1H, ^2J(HH) = 15 Hz, ^2J(HP) = 11 Hz, PC*H*HP], 5.12 [dm, 1H, ^2J(HH) = 15 Hz, PCH*H*P]. Anal. Calcd for $C_{38}H_{22}O_{13}P_3FRu_5$: C, 35.01; H, 1.70. Found: C, 35.57; H, 1.44.

f. Synthesis of $[Ru_5(CO)_{13}(\mu\text{-dppm})(\mu\text{-Cl})(\mu_5\text{-P})]$ (8). The cluster $[Ru_5(CO)_{13}(\mu\text{-dppm})(\mu_4\text{-PN}^i\text{Pr}_2)]$ (**4**; 55 mg, 0.04 mmol) was dissolved in CH_2Cl_2 and treated with HCl (40 μL, 1 M solution in ether, (0.04 mmol) and H_2O (40 μL). The flask was briefly evacuated, refilled with nitrogen, and then allowed to stir for 2 h at room temperature. Over that time, the color changed from green to orange. The solvent was removed in vacuo, and the residue was separated using thin-layer chromatography with hexane as the eluent. Orange crystals of $[Ru_5(CO)_{13}(\mu\text{-dppm})(\mu\text{-Cl})(\mu_5\text{-P})]$ (**8**) were grown from 50:50 CH_2Cl_2/hexane at −30 °C. Yield: 13 mg, 25%. IR (CH_2Cl_2, ν CO, cm^{-1}): 2070 m, 2043 s, 2023 s, 2009 w, 1989 w, 1967 w. $^{31}P\{^1H\}$ NMR ($CDCl_3$): δ 803 [t, ^2J(PP) = 52 Hz], 28 [d, ^2J(PP) = 52 Hz]. ^1H NMR ($CDCl_3$): δ 7.8−7.4 [m, 20H, Ph], 3.73 [dt, 1H, ^2J(HH) = 14 Hz, ^2J(HP) = 11 Hz, PC*H*HP], 3.13 [dt, 1H, ^2J(HH) = 14 Hz, ^2J(HP) = 12 Hz, PCH*H*P]. FAB−MS (m/z): 1322 [M^+], 1294−1069 [$M - nCO]^+$ (n = 1−9). Anal. Calcd for $C_{39}H_{24}O_{13}P_3Cl_3Ru_5$: C, 33.33; H, 1.72. Found: C, 33.76; H, 1.39.

X-ray Analysis. Suitable crystals of compounds **1**·$[H_2N^iPr_2][CF_3SO_3]$, **4**, **5**, **6**, **7**, and **8** were mounted on glass fibers. Diffraction measurements were made on a Siemens SMART CCD automatic diffractometer using graphite-monochromated Mo Kα radiation at −100 °C. The unit cell was determined from randomly selected reflections obtained using the SMART CCD automatic search, center, index, and least-squares routines. Crystal data and collection parameters are listed in Table 4. Integration was carried out using the program SAINT, and an absorption correction was performed using SADABS. Structure solutions were carried out using the SHELXTL 5.1 suite of programs. Initial solutions were obtained by direct methods (SHELXS) and subsequently refined by successive least-squares cycles (SHELXL).

Acknowledgment. This work was supported by the National Research Council of Canada and grants from the Natural Sciences and Engineering Research Council of Canada (to A.J.C.).

Supporting Information Available: Crystallographic data in CIF format for compounds **1** and **4**−**8**. This material is available free of charge via the Internet at http://pubs.acs.org.

IC040077E